ISSN 2229-5518

Design and Experimental Results of a Wavelet Filter for High Performance in Trajectory of Robotic Systems

Jarillo-Silva Alejandro, Domínguez-Ramírez Omar Arturo, Cruz-Tolentino José Alberto, Ramos-Velasco Luis Enrique and Mijangos-Martínez Teresita de Jesús

Abstract -The magnetic permanence servomotors (PM) brushless are reliable devices in motion control applications where a high efficiency, a twisting effort (torque) and speed-torque curves are desired characteristics. Robotics is one of the areas where this type of engines used because of its design features in the development and implementation of electromechanical systems (manipulators). However, a persistent problem in the implementation of the PM motor is persistent variation in the performance of the torque, which generates a signal in riso output thereby generating high frequency signals, which are not desired to pass them directly by motor windings optimum performance and reducing the useful life of the electrical device. The problem is to solve designing digital filters using wavelet theory, designing control laws that allow breaking the inertial effects due to the state of rest and motion and generate optimal trajectories. The filter proposed in this paper has a degree of decomposition of N = 5 and a Buffer size = 128, which is applied to haptic interfaces. However it can be implemented in any electromechanical system. One advantage is that the filter characteristics need not noise signal (cutoff frequency, amplitude).

Index Terms—Chattering, wavelet teory, nonlinear control, trajectories planification.

1 Introduction

TO carry out the implementation of the motion control law is necessary to know the position and velocity of the plant (robot manipulator, conveyor, haptic devices, among other.). For this the use of electric motors with electronic devices equipped to enable processing a signal through a high resolution digital converter called optical encoder are now essential elements in different areas of application, eg industry, home automation, robotics.

Joint position readings are obtained directly in digital format, and also with great accuracy (depending on resolution optical encoder) [1]. To get the speed necessary to articulate the digital data acquired by positioning the optical encoder are processed through mathematical equations, which is considered a minimum time delay $t_r \cong 0$ between reading and processing. The velocity obtained has the same presence of unwanted signals that can be submitted by the low resolution optical encoder, low processing speed and reduced bandwidth[2].

The unwanted signals (noise) alter the form factor of the original signal to generate changes in amplitude. Moreover nonlinear control law using the speed signal as part of the articular nominal reference $\dot{q}_r = \dot{q}_d + \alpha\tilde{q}$, where $\dot{q}_d$ represents the vector of desired joint velocities, α determines a positive definite symmetric matrix and finally $\tilde{q} = q - q_d$ represents the joint error vector [3]. The nominal reference $\dot{q}_r$ is explicitly in the sliding surface $s(\tilde{q}, t) = \dot{q} - \dot{q}_r$ with the same form factor of the noise signal, and therefore generate electrical noise in the motor windings, obstructing them a good tracking paths to a high sampling rate. In addition, delays in reading position and velocity errors cause, same as increasing the degree of instability during follow a path, where the behavior of the end effector of the device is affected due to the electrical impulses generated by the control law.

1.1 Justification

Any electric motor which does not have a device which allows its position and angular velocity, it is possible through the rotation axis of an optical encoder coupled. The optical encoders act as transducers feedback same as those used for the implementation of a velocity control and/or position. An advantage of implementing optical encoders corresponds to the partial elimination of electrical noise generated by the windings of the motor, however it is the presence of white noise. The level of resolution that introduces an optical encoder does not solve the problem, for example, the speed reading obtained from one of the optical encoders PHANToM 1.0 haptic device is presented in Figure 1 and although the resolution is still 1Khz noise exist. The causes which determine the noise factor can be varied, for example, temperature, switching on the motor torque, magnetic flux, and so on. There are several alternatives to eliminate the noise generated in electric motors, for example, the design and implementation of analog filters, which are composed of active and passive electrical elements (resis-

- *Jarillo-Silva Alejandro, Cruz-Tolentino José Alberto and Mijangos-Martínez Teresita de Jesús, University of the Sierra Sur, México, Oaxaca, E-mail: ajarillo, jacruz,tmijangos@unsis.edu.mx*
- *Domínguez-Ramírez Omar A., Ramos-Velasco Luis E., Autonumos University of Hidalgo State, Hidalgo, México. E-mail: omar@uaeh.edu.mx*

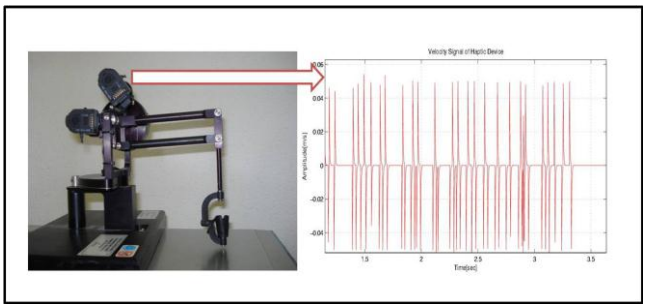

Fig. 1. Velocity signal obtained from reading the optical encoders PHANToM 1.0 haptic device.

tors and capacitors mainly) and depending on the filter order increases the number of elements[4]. Another method involves the design of digital filters by means of programming, which excludes the use of electronic elements to reduce noise. However, it requires more computational resources to implement it. It is also well known that the noise signal is characterized by high frequency, low amplitude (see Fig 1). The complexity is high when attempting to characterize the noise signal and velocity, that in some cases, make difficult the task to design a digital filter, which achieves the necessary requirements to perform filtering. In recent studies [2] has shown that one way to solve the noise problem is to implement an adaptive control law, which consists of a filter with PD action instead of a conventional PD, this significantly reduces the harmonic content of the efforts of mechanical torque joints. In [5] and [6] schemes are described for estimating the value of the velocities using observers, but its application requires a high computational effort.

1.2 Purpose

Design and implement digital filters based on wavelet theory that can adapt to any electromechanical system that uses one or more actuators. The filter should reduce noise introduced in the signal obtained by the optical encoder of the actuator without the need to characterize. Furthermore in order to generate a smooth trajectory of movement that does not generate noise during follow-up to this technique is proposed to use the RGB (Regulation Based Monitoring)[7]. This paper proposes the design of a wavelet filter, it is implemented in the haptic device PHANToM 1.0, which is applied a nonlinear control law based on sliding mode theory, Euler-Lagrange and passivity with position feedback and joint speed.

2 Review of Some Control Laws for Robotic Manipulators

Consider a mechanism of articulate links (PHANToM 1.0), with n revolute joints described in generalize joint coordinates . Physically, the robot is never in touch with a physical object, thus robot dynamics in free motion describe properly the haptic device, as follows

$$D(q)\ddot{q}+C(q,\dot{q})\dot{q}+G(q)+B(q,\dot{q})=\tau \qquad (1)$$

Where $D(q) \in \mathbb{R}^{3x3}$denotes a symmetric positive definite inertial matrix, $C(q,\dot{q}) \in \mathbb{R}^{3x3}$ is a Coriolis and centripetal forces matrix, $G(q) \in \mathbb{R}^{3x1}$ models the gravity forces vector, denotes a symmetric positive definite viscous coefficient matrix, and stands for the torque input. In our case the human operator is driving the system, therefore $\tau = \tau_c + \tau_h$ and stands for the guidance control, and denotes the human-haptic interaction, where stands the transpose Jacobian of the haptic device, and represent the human performance force vector.

2.1 Joint control law based on passivity

To achieve these objectives is necessary to design a control strategy based on sliding mode theory of second order, to present robustness. In order to ensure the stability of the system are used Lyapunov theory (second method), passivity property and the dynamic error property. The control strategy is as follows [8].

$$\tau = -K_{ds}s - K_L \int \tanh(s)ds \qquad (2)$$

Where K_{ds} *and* K_L are arrays of the same dimensions, diagonal and positive definite, $s = \dot{\tilde{q}} + \alpha\tilde{q}$ defined the dynamic error, $\dot{\tilde{q}} = \dot{q} - \dot{q}_d$ and $\tilde{q} = q - q_d$ where $(q, \dot{q})$ are current joint positions and velocities, $(\tilde{q}, \dot{\tilde{q}})$ represent the desired joint positions and velocities with the same dimensions. Finally τ can also be defined as $\tau = J^T F$ determines the torque vector, where J^T corresponds to the transposed Jacobian matrix of the robotic system and is the force that is used in the motors of the robotic system. Obtaining the force vector has to be $F = J^{T^{-1}}\tau$, this indicates that the engines force is directly proportional to the Jacobian matrix. Moreover, it is well known that the armature current i_a MP engine DC is directly related linearly with the control signal due to τ is also described as $\tau = K_t i_a$, where k_t is the constant of reinforcement provided by the manufacturer (see Fig. 2).

The armature current signal is defined by the control signal thus has the same form factor described by amplitude and frequency. Therefore because the control signal depends on the presence of noise signals, electrical and mechanical stresses are greatest decrease causing the useful life of the system elements. The following section presents a possible solution to the problem using different techniques.

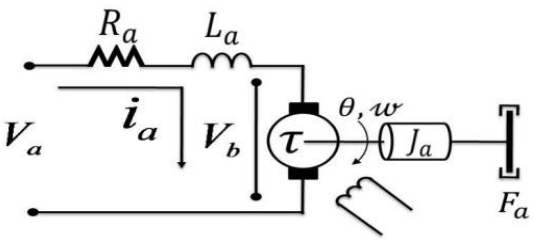

Fig. 2. Velocity signal obtained from the optical encoders PHANToM 1.0 haptic device.

3 WAVELET FILTER DESIGN

Wavelets have been used to analyze signals at different scales [9]. These are applied in systems where a signal is required to analyze cumulative effects in this uncertainty, for example, change unwanted signals generated by mechanical vibration, external disturbances. Such signals are expressed in different frequency ranges. To analyze these signals using wavelet theory allows decomposition of the signal. Thus undesired signals can be eliminated. In this section is designed to velocity wavelet filter in order to reduce signal noise induced into the articular velocity.

3.1 Wavelet Theory and Multiresolution Analysis

Here, we briefly summarize some results from the wavelet theory that are relevant to this work, for it we use the notation presented in the Table 1.

A wavelet is defined as an oscillatory wave Ψ of very short duration and satisfy the admissibility condition,

TABLE 1
NOTATION

$\psi(t)$	Mother wavelet function
$\psi_{a,b}$	Daughter wavelet function
$W_f(a,b)$	Continuous wavelet transform
$W_f[a,b]$	Discrete wavelet transform
$< f,g >$	Inner product between f and g
$\oplus$	Direct sum of subspaces
$V \perp W$	V is orthogonal to W
$L^2(\mathbb{R})$	Vector space of all measurable, square integrable functions
$\mathbb{R}$	Vector space of the real numbers
$\mathbb{Z}$	Set of all integers

given by

$$\Psi(0) = \int_{-\infty}^{\infty} \psi(t)dt = 0 \tag{3}$$

Where Ψ is the Fourier transform of wavelet function ψ, the latter also called wavelet mother function, the mathematical representation of some mother wavelet are shown in Table 2 their graphs are plotted in Fig. 3. Wavelet function Ψ is called the "mother wavelet" because different wavelets generated from the expansion or contraction, and translation, theycalled "daughter wavelets", which have the mathematical representation given by:

$$\psi_{a,b}(t) = \frac{1}{\sqrt{a}}\psi\left(\frac{t-b}{a}\right),\ a \neq 0; a,b \in \mathbf{R} \tag{4}$$

Where a is the dilation variable that allows for the expansions and contractions of the Ψ and b is the translation variable and allows translate in time. There are two types of wavelet transform: continuous wavelet transform (CWT) and discrete wavelet transform (DWT), whose mathematical definition are given by (3) and (4), respectively

$$\psi_{a,b}(t) = \frac{1}{\sqrt{a}}\psi\left(\frac{t-b}{a}\right),\ a \neq 0; a,b \in \mathbf{R} \tag{5}$$

for CWT, the expansion parameters a and translation b vary continuously on $\mathbb{R}$, with the restriction $a > 0$. For DWT, the parameters a and b are only discrete values: $a = a_0^m$, $b = kb_0a_0^m$ where $a_0 > 1$, b_0 and are fixed values.

$$W_f[a,b] = \frac{1}{\sqrt{a_0^m}}\int_{-\infty}^{\infty} f(t)\psi\left(\frac{t}{a_0^m} - kb_0\right)dt \tag{6}$$

In DWT, one of the most important feature is the multiresolution analysis. Multiresolution analysis with a function $f \in L_2(\mathbb{R})$, can be decomposed in the form of successive approximations, using wavelet basis functions. The

TABLE 1
SOME EXAMPLES OF COMMON MOTHER WAVELETS

Haar	$\psi(t) = \begin{cases} 1, \text{ if } t \in [0, \frac{1}{2}] \\ -1, \text{ if } t \in (\frac{1}{2}, 1] \\ 0, \text{ otherwise} \end{cases}$
Mexican hat	$\psi(t) = \frac{2}{\sqrt{3}}\pi^{-\frac{1}{4}}(1-t^2)e^{(-\frac{1}{2}t^2)}$
Morlet	$\psi(t) = e^{-\frac{t^2}{2}}cos(5t)$
Shannon	$\psi(t) = \frac{sin(\frac{3\pi}{2}t)}{\frac{3\pi}{2}t}cos(\frac{3\pi}{2})t$
Daubechies	$P(y) = \sum_{k=0}^{N-1} C_k^{N-1+k}\, y^k$; C_k^{N-1+k} are binomial coefficients, N is the order of the wavelet
Meyer	$\psi(\omega) = \begin{cases} \frac{e^{\frac{i\omega}{2}}}{\sqrt{2\pi}}\sin(\frac{\pi}{2}v(\frac{3}{2\pi}\lvert\omega\rvert - 1)), \\ \text{if } \frac{2\pi}{3} \le \lvert\omega\rvert \le \frac{4\pi}{3} \\ \frac{e^{\frac{i\omega}{2}}}{\sqrt{2\pi}}\cos(\frac{\pi}{2}v(\frac{3}{4\pi}\lvert\omega\rvert - 1)), \\ \text{if } \frac{4\pi}{3} \le \lvert\omega\rvert \le \frac{8\pi}{3} \\ 0, \text{ otherwise} \end{cases}$ $v = a^4(35 - 84a + 70a^2 - 20a^3)$, $a \in [0,1]$

multiresolution analysis consists of sequence su cessive approximations of enclosed spaces, nested spaces $\{V : N \in \mathbb{N}\}$ with the following properties:

$$V_j \subset V_{j-1},\ \forall j \in \mathbf{Z} \tag{7}$$

$$\bigcup_j V_{j\in} = L_2(\mathbf{R}) \tag{8}$$

$$\bigcap_j V_{j\in} = \{0\} \tag{9}$$

Given a function $f[n]$, define as:

$$f[n] \in V_0 \Leftrightarrow f[n-k] \in V_0,\ \forall k \in \mathbf{Z} \tag{10}$$

And given a function $\phi[n] \in V_o$, called scaling function, such as:

$$\phi_{j,k}[n] = 2^{-\frac{j}{2}}\phi[2^{-j}n - k],\ \forall j,k \in \mathbf{Z} \tag{11}$$

Forming an orthogonal basis V_o, from $\phi[n]$ is possible V_o, if for each V_j exist a complementary space W_j that meets the following conditions

$$V_{j-1} = V_j \oplus W_j \tag{12}$$

$$V_j \perp W_j = 0, \forall j \in \mathbf{Z} \tag{13}$$

and either

$$\psi_{j,k}[x] = 2^{\frac{-j}{2}} \psi[2^{-j}x - k], \forall j,k \in \mathbf{Z} \tag{14}$$

From the above we can say that the purpose of analysis multiresolution is to determine a function $f[n]$ by successive approximations, as

$$f[n] = \sum_{k=-\infty}^{\infty} c_{N,k}\phi_{N,k}[n] + \sum_{m=1}^{N}\sum_{k=-\infty}^{\infty} d_{m,k}\psi_{m,k}[n] \tag{15}$$

With

$$c_{m,k} = \sum_{k=-\infty}^{\infty} f[n]\overline{\phi_{m,k}[n]} \tag{16}$$

$$d_{m,k} = \sum_{k=-\infty}^{\infty} f[n]\overline{\psi_{m,k}[n]} \tag{17}$$

Where N is the level at which decomposes $f[n]$ and φ[n], ψ[n] are conjugate functions for φ[n] and ψ[n], respectively. Multiresolution analysis, in addition to being intuitive and useful in practice, forms the basis of a mathematical framework for wavelets. One can decompose a function a soft version and a residual, as we can see from (9), where the wavelet transform decomposes a signal $f[n]$ in one approach or trend coefficients c and detail coefficients d which, together with φ [n] and ψ[n], are the smoothed version and the residue, respectively.

An efficient approach for multiresolution analysis is to use the coding scheme sub-band, which uses only the filters $h[k]$ and $g[k]$, which and are related as follows

$$h[k] = \sqrt{2}\sum_x \phi[x]\overline{\phi[2x-k]} \tag{18}$$

$$g[k] = \sqrt{2}\sum_x \psi[x]\overline{\psi[2x-k]} \tag{19}$$

$$g[x] = (-1)^k \overline{h[-k+1]} \tag{20}$$

Fig. 4 and Fig. 5 shows the decomposition analysis and synthesis of decomposition of a signal f[n] by a coding scheme subband, respectively.

Figure 3 shows as $f[n]$ a signal enters a pair of filters, where one of them is $\overline{h[k]}$ low pass and high pass the other is $\overline{g[k]}$ (which are conjugates filters h[k] and g[k]), which handle half the width of band of the input signal $f[n]$. The symbol ↓ 2 represents the operation of two decimation (down sampling), ie taking the first data, removes the second data, takes the third data and fourth data is eliminated, and so on. The low pass filter output sent back to another pair of filters of the same characteristics. Thus will reduce the bandwidth of the signal and this results in a halving of the resolution. This means that a larger number of filter stages will have a higher resolution.

Fig. 5 shows the process to recover the signal from the decomposition analysis, now in reverse. The symbol ↑ 2 represents the operation of interpolation to two (up sampling), ie data are inserted between each data value zero of the signal to be interpolated. Subsequent to the output signal of each filter are summed at each level of synthesis to completely recover the original signal or part thereof

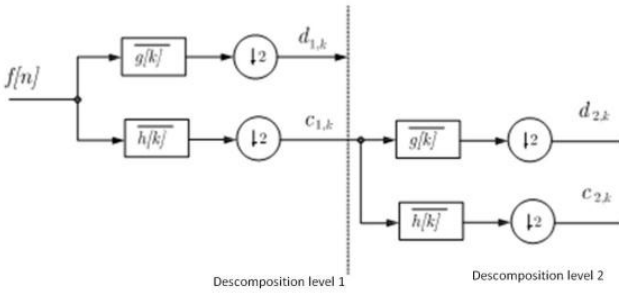

Fig. 4. Analitys of the descomposition signal f[n].

without the original signal components of signals.

3.2 Design of Wavelet Digital Filter

A wavelet filter is implemented based on the analysis multiresolution, considering that (15) to decompose a signal $f(x)$ a a resolution level N, the result of this decomposition in a high level signal (low frequency) and N signals of medium and low scale (medium and high frequency). Considering the low level signal as a noise signal, it is possible to consider $f(x) = C_0$, which decomposes in two signal C_1 and D_1, where C_1 define a low

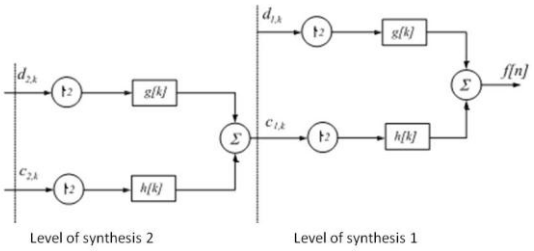

Fig. 5. Synthesis of decomposition of the signal f[n].

frecuency signal and D_1 determined a hight frecuency signal, therefore a signal $f(x)$ with a decomposition level 1 without low level signal is as shown in Fig. 6.

C_1 signal can still be infinitely decomposing to C_N, where N is the level of decomposition. The higher the level of decomposition, the signal $f^*(x)$ is better filtered

$$f[n] = \sum_{k=-\infty}^{\infty} c_{N,k}\phi_{N,k}[n] + \sum_{m=1}^{N}\sum_{k=-\infty}^{\infty} d_{m,k}\psi_{m,k}[n] \tag{21}$$

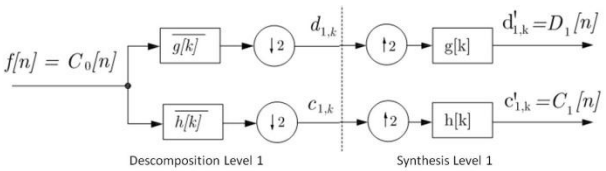

Fig. 6. Decomposition diagram of a signal $f(x) = C_0$

4 EXPERIMENTS AND RESULTS

4.1Implementation

The experimental platform used in this work for the evaluation of digital filter design corresponds to the haptic device PHANToM Premium 1.0 has three degrees of freedom, consists of three brushless motors MP. The haptic device generates kinesthetic feedback (linked with muscles and tendons) due to the absence of a force sensor on the end effector.

4.2 Trayectory Planning

Trajectory planning is performed in a wide working space of the haptic device, so that areas approaching unique. For this case it is necessary to generate a path in much of the allowable workspace haptic device PHANToM premium1. For this reason the task is divided into two different paths.

The first path is represented by the fifth degree polynomial $\xi(t) \in \mathbf{R}$. Such important features in this polynomial are reflected in the performance of the haptic device, for example, early breaks with the inertial effects due to the idle state of the device, and finally breaks the inertial effects due to the state of motion of the haptic device, thus forming a bell shaped curve, where precisely at half maximum velocoty is reached as shown in Fig. 6 the equation which defines in (22). Considering the following initial conditions$\xi(t_0) = 0$, $\xi(t_b)$ and $\ddot{\xi}(0.5t_b)$. Solving the system of equations is obtained$a_3 = 10$, $a_4 = 15$ and $a_6 = 6$ [8].

$$\xi(t) = a_3\frac{(t-t_0)^3}{(t_b-t_0)^3} - a_4\frac{(t-t_0)^4}{(t_b-t_0)^4} + a_5\frac{(t-t_0)^5}{(t_b-t_0)^5}$$

$$\dot{\xi}(t) = 3a_3\frac{(t-t_0)^2}{(t_b-t_0)^3} - 4a_4\frac{(t-t_0)^3}{(t_b-t_0)^4} + 5a_5\frac{(t-t_0)^4}{(t_b-t_0)^5} \qquad (22)$$

$$\ddot{\xi}(t) = 6a_3\frac{(t-t_0)}{(t_b-t_0)^3} - 12a_4\frac{(t-t_0)^2}{(t_b-t_0)^4} + 20a_5\frac{(t-t_0)^3}{(t_b-t_0)^5}$$

The second path consists of a circumference, which is

$$\begin{aligned} x &= h + r\cos(wt) \\ y &= 0.03 \\ z &= k + r\sin(wt) \end{aligned} \qquad (23)$$

Where (h,k) represents the coordinates of the circumference center, and r define the radius. For this case study h=0, k=0 and r=0.02m. The derivatives with respect to

$$\begin{aligned} \dot{x} &= -rw\sin(wt) \\ \dot{y} &= 0 \\ \dot{z} &= rw\cos(wt) \end{aligned} \qquad (24)$$

Where $w = 2\pi f$ and $f = 0.1$. Finally $t = 9sec$, in the Fig 7

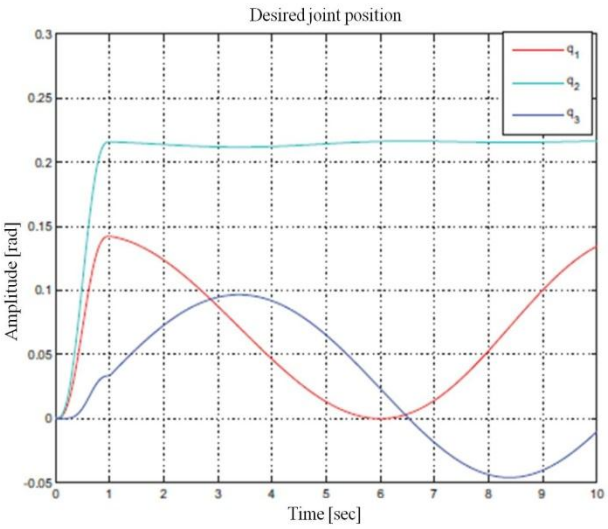

Fig. 7. Desired joint position of the differents haptic device links.

showed the workspace.

The task consists of two paths. The first is determined by the polynomials (22) where $t_0 = 1$. In Fig 7 is presented the joint path of the task, which has a duration of 1 second. In this path the haptic device end effector is moved to the starting point of the circumference, so that after performing the second path, which is defined by the parametric equations of a circle, with a time of 9 seconds.

In Fig 8 shows the desired joint velocity of the task. At time 0 to 1 shows the waveform of the gears, which have bell-shaped, where exactly half of the trajectory is reached maximum velocity, and it begins to decrease as he approaches the reference point breaking this inertial effects due to the state of motion. Finally in the Fig. 9 is present

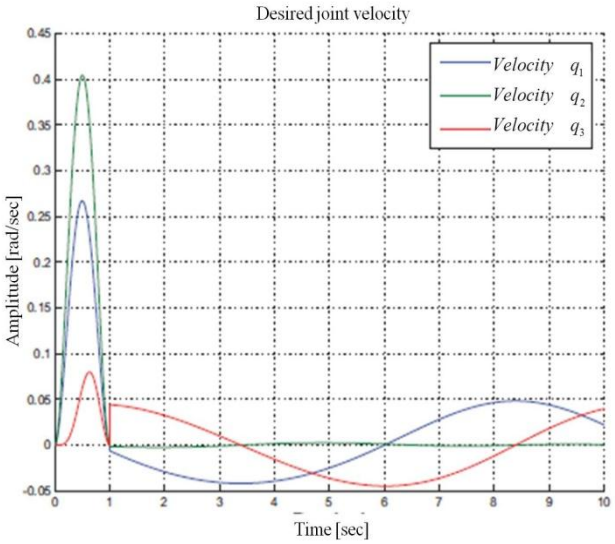

Fig. 8. Desired joint velocity of the haptic device links.

the desired trajectory on workspace.

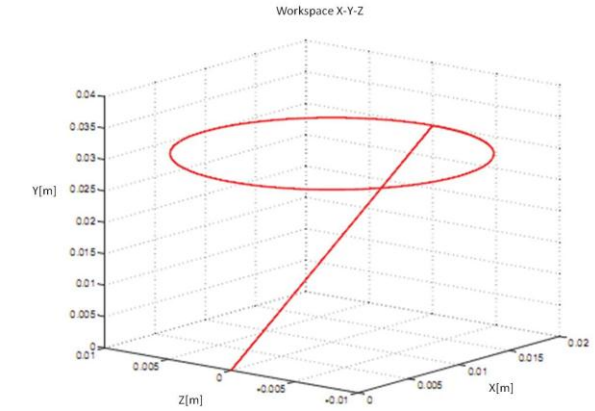

Fig. 9. Trajectory planning in the haptic device workspace.

4.3Implementation

To perform the experiments used a wavelet filter with a velocity resolution level with coefficients N = 5 Daubechies m = 7. In Figure 10 shows the diagram of the filter.

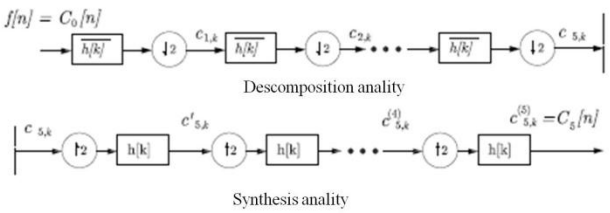

Fig. 10. Wavelet filter diagram.

The control law used corresponds to nonlinear control theories badaso in sliding mode and passivity presented in (2). In Fig 11, 12 and 13 show the velocity obtained by the optical encoders and velocity filtered. The wavelet filter eliminates the high values of the velocity signal, thereby achieving low amplitude control signal, and therefore low values in the the motor voltage.

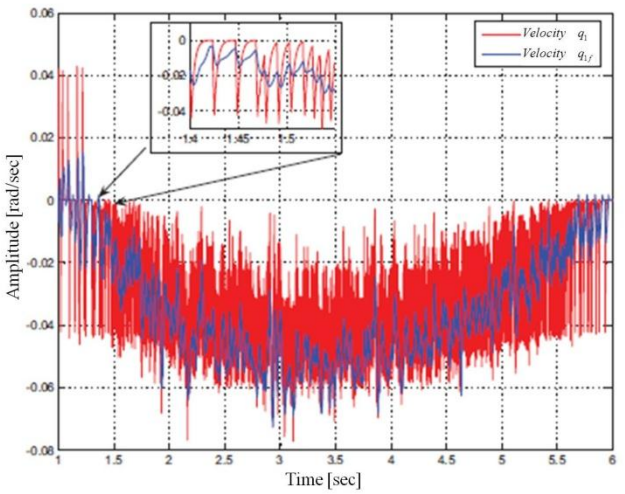

Fig. 11 Joint velocity signal filtered vs joint velocity q1 of the haptic device.

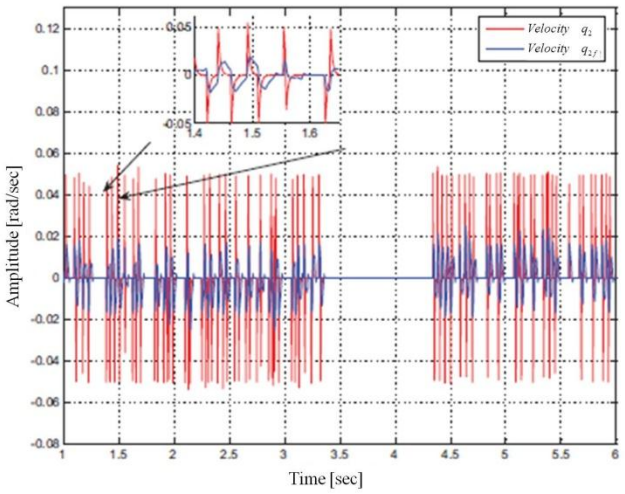

Fig. 12 Joint velocity signal filtered vs joint velocity q2 of the haptic device.

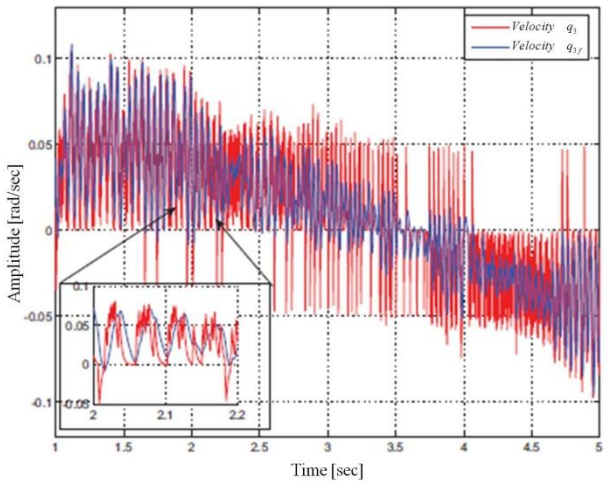

Fig. 13 Joint velocity signal filtered vs joint velocity q3 of the haptic device.

4.3Discusions

In contrast speed signals filtered and unfiltered displayed significant variation as to the presence of noise. Moreover the implementation of a digital filter wavelet, and the use of a nonlinear control and path planning within the allowable working space being excellent combinations are possible to obtain efficient performance haptic device.

Noise signals are generally of low amplitude but high frequency distortion generated and altered in any form factor signal as oberva in fig. 11,12 and 14. The major application of the filter is not required since the signal characterizing this gives a new way to filter any signal. Descomposión level is relevant as to decompose the signal into N signals, which are analyzed by themselves different wavelets for exclusion in the synthesis of the filtered signal.

4 CONCLUSION

The problem of characterizing a signal that varies with respect to time is difficult in some cases. Furthermore, if the signal is present it is difficult to achieve chaterring characterize the signal. In robotic systems, the presence of these signals is common due to disturbance signals that are latent. Furthermore electrical noises signals and disrupt mechanical velocity and position signals.

The wavelet theory is a possible solution considering that does not require the characterization of the signal. On the other hand the control signal plays an important role as the planning of the task, since it relies heavily on the robotic system to perform a task free of noise.

The computational cost required to implement the digital filter algorithm compensates the excellent performance of the haptic device. Achieving increase the lifetime of the electrical and mechanical machines.

ACKNOWLEDGMENT

Thank CINVESTAV Saltillo unit layout PHANToM 1.0 haptic device. Also appreciate the cooperation of haptic interfaces Laboratory of the University of the Sierra Sur.

REFERENCES

[1] Alex Seguritan, Max Rotunno, "Torque Pulsation Compensation for DC Motor using an Extended Kalman Filter Approach", *Proceedings of the 41st IEEE, Conference on Decision and Control*, Las Vegas, Nevada USA, pp. 486-491, December 2002.

[2] F. Alonge, T. Raimondi and F. DIppolito, "Velocity Estimation by Digital Filtering of Position Data to Process Adaptive Control Laws for Robotics Manipulators", *Proceedings of the 1996 IEEE IECON 22nd International Conference on, 5-10*, Aug 1996.

[3] Jean-Jacques E. Slotine Weiping Li, "Applied Nonlinear Control," Prentice Hall, USA, pp. 276-300, 1991.

[4] Albert Paul Malvino, "Electronics Principles", José Rioga, McGraw-Hill, Madrid, pp.767-797, 1993.

[5] S.Nicosia, P.Tomei, "Robot Control Using Only Joint Position Measurements", *IEEE Trans. on AC*, Vol. 35, N. 9, pp. 1058-1061, September, 1990.

[6] M. Erlic, W. S. Lu, "A Reduced-Order Adaptive Velocity Observer for Manipulator Control", *IEEE Trans. on AC*, Vol. 11, N. 2, April, 1995.

[7] Domínguez Ramírez O, Parra Vega V, Díaz Montiel M, Poza Cárdenas M and Hernández Gómez R, "Cartesian Sliding PD Control Of Robot Manipulator for Tracking in Finite Time: Theory and Experiments, Chapter 23 in DAAAM international Scientific Book 2008, pp. 257-272, B. Katalinc (Ed.), Published by DAAAM international, Vienna, Austria 2008.

[8] A. Jarillo-Silva, O.A Domínguez-Ramírez and V.Parra-Vega, "Joint Control Strategy for Haptic Guidance", *2010 Electronics, Robotics and Automotive Mechanics Conference*, pp. 411-416, Septiembre, 2010.

[9] S. Mallat, "A Theory Multiresolution Signal Descomposition: The Wavelet Transform",*IEEE Trans. Pattern. Annal. Machine Intell*, pag. 674-693, 1989.